Journal of Power Sources 196 (2011) 10737–10747

Contents lists available at SciVerse ScienceDirect

Journal of Power Sources

journal homepage: www.elsevier.com/locate/jpowsour

Dynamic modelling of the effects of ion diffusion and side reactions on the capacity loss for vanadium redox flow battery

Ao Tang, Jie Bao, Maria Skyllas-Kazacos*

School of Chemical Engineering, University of New South Wales, Sydney, NSW 2052, Australia

ARTICLE INFO

Article history:
Received 27 May 2011
Received in revised form 30 August 2011
Accepted 1 September 2011
Available online 7 September 2011

Keywords:
Vanadium redox flow battery
Dynamic modelling
Capacity loss
Ion diffusion
Side reactions

ABSTRACT

The diffusion of vanadium ions across the membrane along with side reactions can have a significant impact on the capacity of the vanadium redox flow battery (VFB) over long-term charge–discharge cycling. Differential rates of diffusion of the vanadium ions from one half-cell into the other will facilitate self-discharge reactions, leading to an imbalance between the state-of-charge of the two half-cell electrolytes and a subsequent drop in capacity. Meanwhile side reactions as a result of evolution of hydrogen or air oxidation of V^{2+} can further affect the capacity of the VFB. In this paper, a dynamic model is developed based on mass balances for each of the four vanadium ions in the VFB electrolytes in conjunction with the Nernst Equation. This model can predict the capacity as a function of time and thus can be used to determine when periodic electrolyte remixing or rebalancing should take place to restore cell capacity. Furthermore, the dynamic model can be potentially incorporated in the control system of the VFB to achieve long term optimal operation. The performance of three different types of membranes is studied on the basis of the above model and the simulation results together with potential operational issues are analysed and discussed.

1. Introduction

The vanadium redox flow battery has been considered to be one of the most promising large scale energy storage systems that can be combined with renewable energy sources such as solar and wind energy for electrical energy storage and distribution [1–4]. Compared with conventional rechargeable batteries, the VFB stores energy in the form of two vanadium solutions contained in two separate electrolyte reservoirs, thereby enabling the battery capacity to be readily increased by simply adding more solution. In addition, the power output is determined by adjusting the number of cells and the electrode area. As vanadium ions are employed in both half-cells, the issue of cross-contamination during long term use is eliminated, so that the electrolyte has an indefinite life. With its excellent features and flexibility, a number of applications have been successfully field tested in different parts of the world in areas such as peak shaving, load levelling, emergency back-up, as well as renewable energy output smoothing. During operation of the VFB, the electrolyte is pumped through pipes from the tanks into the cells where the following reactions occur.

At positive electrode:

$$VO^{2+} + H_2O \underset{\text{discharge}}{\overset{\text{charge}}{\rightleftarrows}} VO_2^+ + 2H^+ + e^-, \quad E^0 = 1\,V \tag{1}$$

At negative electrode:

$$V^{3+} + e^- \underset{\text{discharge}}{\overset{\text{charge}}{\rightleftarrows}} V^{2+}, \quad E^0 = -0.26\ V \tag{2}$$

One of the essential parts of the VFB is the membrane through which the charge is balanced by the movement of hydrogen ions during charging and discharging. The ideal membrane should have low permeability to vanadium ions, high proton conductivity, good chemical stability in acid solution, good mechanical integrity as well as low cost. To date many types of membrane have been successfully evaluated for use in the VFB [5–12] and some of these have been applied in both demonstrations and commercial systems [13–15], while further investigation and development of new membranes for cost reduction have been also reported [16–18]. Nevertheless, as with all electrochemical energy storage systems, self-discharge and side reactions will occur and reduce capacity during long-term cycling.

In the case of the VFB, self-discharge reactions are mainly associated with the diffusion of vanadium ions from one half-cell to the other due to the concentration gradients of each of the ions across the membrane. This will give rise to a reduction in the coulombic efficiency, the magnitude of which will depend on the

* Corresponding author. Tel.: +61 2 9385 4335; fax: +61 2 9385 5966.
E-mail address: m.kazacos@unsw.edu.au (M. Skyllas-Kazacos).

0378-7753/$ – see front matter © 2011 Elsevier B.V. All rights reserved.
doi:10.1016/j.jpowsour.2011.09.003

diffusion rates of the vanadium ions across the particular membrane. Many researchers have already focused on the self-discharge behaviour for different types of membranes in the VFB. Early studies by Skyllas-Kazacos and co-workers reported the properties of a wide range of anion and cation exchange membranes in small VFB single cells [5–15] and found that the magnitude and direction of water and vanadium ion transfer depends on the state-of-charge of the solutions and the properties of the membrane (including ion exchange capacity and type of ion exchange groups–anionic vs. cationic). The group proposed a number of membrane treatment processes to reduce the magnitude of water and electrolyte transfer in order to minimise operational problems and capacity loss during long-term operation of the VFB. No membrane or treatment process can, however, totally eliminate the transfer of vanadium ions and water from one half-cell to the other, so some capacity loss will always be observed during long-term cycling. Apart from diffusion effects, side reactions such as evolution of hydrogen at the negative electrode during charging and air oxidation of V^{2+} in the negative electrolyte solution will also influence capacity loss by disturbing the molar ratio of the charged to discharged species in the two half-cells. All these factors exist in the VFB systems and cause imbalance among the vanadium ions of different states of oxidation, thereby leading to a deteriorative capacity performance during long term use. A dynamic model that can be used to simulate these phenomena and predict their effect on battery capacity would be invaluable in the development of sophisticated control systems for the VFB.

In recent years, mathematical models of the VFB have been developed to predict and investigate the performance of the VFB systems [19–25]. Walsh and co-workers [19–22] developed a transient two-dimensional model based on conservation principles combined with a global kinetic model for reactions to simulate the performance of the VFB with respect to variations in parameters. It was further extended to include effects of temperature variation and several side reactions. Li and Hikihara [23] proposed a simple dynamic model suitable for control purpose on the basis of physical phenomena and chemical kinetics. To date, no dynamic models of the VFB, however, have been developed to describe capacity loss caused by vanadium ion diffusion and side reactions. In this paper, a dynamic model based on the conservation of mass is developed to study the charge–discharge cycling capacity loss caused by the diffusion of vanadium ions across the membrane as well as side reactions. Such a model will be useful for developing battery control systems that can automatically restore the capacity of the VFB by rebalancing the electrolytes after long term operation. Moreover, the Nernst Equation is used in conjunction with the mass balance model to produce a dynamic model of the cell voltage that can predict the capacity of the cell for long term charge–discharge cycling under specific operating limits of cell voltage. The prediction of capacity can help with making decisions for the implementation of periodic electrolyte rebalancing to equalize the vanadium ion concentrations in both electrolyte tanks and thereby restore capacity during operation. Simulations have been performed to investigate the capacity loss for different types of membranes and different levels of hydrogen evolution and air oxidation during long term charge–discharge cycling operation.

2. Effects of diffusion and side reactions

The membrane in the VFB plays an important role in separating the positive and negative half-cell electrolytes containing pentavalent/tetravalent and bivalent/trivalent vanadium ions respectively within the cell. It allows hydrogen ions to go through the membrane in order to balance the charge while preventing the transfer of vanadium ions from one half-cell to the other. In reality,

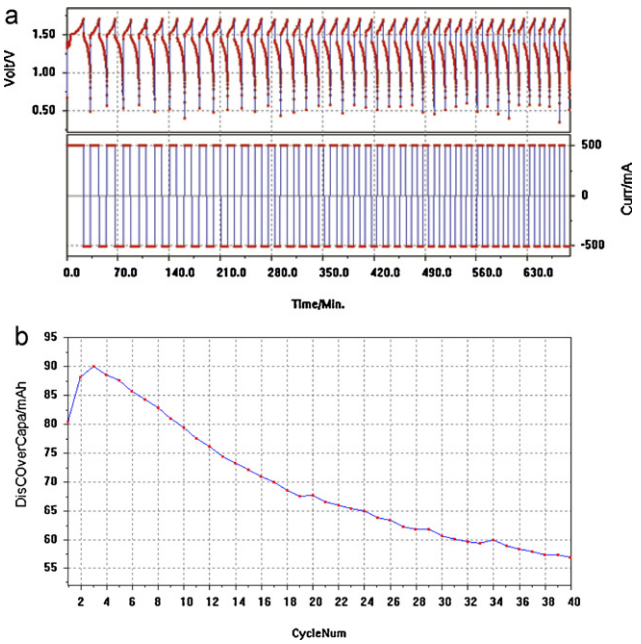

Fig. 1. Performance of a small static cell employing perfluorinated cation exchange membrane. (a) Voltage and current vs. time during charge–discharge cycling. (b) Capacity vs. cycle number.

however, the crossover of vanadium ions through the membrane cannot be entirely avoided due to the fact that diffusion always occurs when there is the concentration difference of vanadium ions existing between the positive and negative half-cell electrolytes. This gives rise to self-discharge reactions in each electrolyte and a subsequent loss of capacity. With regard to ion diffusion, all the vanadium ions in four different states of oxidation undergo diffusion across the membrane and react with each other causing reactions shown as follows.

In the positive half-cell, diffusion of V^{2+} and V^{3+} ions from the negative half-cell will lead to the following self-discharge reactions:

$$V^{2+} + 2V^{5+} \rightarrow 3V^{4+} \quad (3)$$

$$V^{3+} + V^{5+} \rightarrow 2V^{4+} \quad (4)$$

$$V^{2+} + V^{4+} \rightarrow 2V^{3+} \quad (5)$$

while in the negative half-cell, V^{5+} and V^{4+} ions from the positive side will react as follows:

$$V^{5+} + 2V^{2+} \rightarrow 3V^{3+} \quad (6)$$

$$V^{4+} + V^{2+} \rightarrow 2V^{3+} \quad (7)$$

$$V^{5+} + V^{3+} \rightarrow 2V^{4+} \quad (8)$$

According to the above self-discharge reactions, an imbalance in vanadium ions will occur in the two half-cells if the diffusion rates of the different vanadium ions are not equal. This would lead to a build up of vanadium ions in one half-cell and a corresponding decrease in the other, thus giving rise to loss of capacity. This phenomenon is demonstrated in Fig. 1a that shows the laboratory cycling test charging–discharging current and cell voltage curves generated from a small sealed static cell employing a perfluorinated cation exchange membrane. A small current density of 20 mA cm^{-2} was employed in order to minimise the evolution of hydrogen during charging, while the sealed cell prevented any air ingress that would cause oxidation of V^{2+}. A gradual decrease of capacity can be observed in 40 charge–discharge cycles in Fig. 1b, which is mainly attributed to the differential rates of diffusion of the vanadium ions

from one half-cell to the other. Such capacity loss can be readily restored by simply remixing the two electrolytes in order to rebalance the vanadium concentrations in each half-cell.

The above effects of vanadium ion diffusion across the membrane can be established by means of Fick's first law shown below which describes that the flux of diffusion is from region of high concentration to region of low concentration with a magnitude proportional to the concentration gradient.

$$J = -k\frac{dc}{dx} \tag{9}$$

where J is the flux of diffusion ($\mathrm{mol\,L^{-1}\,s^{-2}}$), k is the diffusion coefficient ($\mathrm{ms^{-1}}$), dc is the concentration difference across the membrane ($\mathrm{mol\,L^{-1}}$) and dx is the diffusion layer thickness which is assumed to be equal to the thickness of membrane (m).

During the process of charging, however, gassing side reactions can occur at both electrodes, giving rise to a loss in coulombic efficiency. While oxygen evolution at the positive electrode has been shown to be negligible up to relatively high states-of-charge (SOC), hydrogen evolution at the negative electrode can be quite significant above 90% SOC. For this reason, the practical operating range of the VFB is usually set between 10% and 90% SOC. Any difference between the rates of the two gassing reactions will, however, give rise to an imbalance between the SOCs of the two electrolytes that can in turn have a remarkable impact on cell capacity. For example, if 1% of the charging current is consumed by hydrogen evolution at the negative electrode, this will lead to a 1% loss of capacity at each cycle and 100% capacity loss after only 100 cycles.

As mentioned above, a second side reaction that will lead to further capacity loss is air oxidation of bivalent vanadium ion in the negative half-cell electrolyte. This will also lead to an imbalance between the V^{2+} and V^{5+} ions in the two half-cells thus reduce capacity. The effect of these processes on cell capacity is illustrated in Fig. 2, which shows the charge–discharge voltage profiles for a small laboratory flow cell with open electrolyte reservoirs was cycled at a relatively larger current density of 40 mA cm^{-2}. From Fig. 2b it can be seen that the capacity decreased from 800 to 120 mAh over only 20 cycles, considerably more than the capacity loss observed in the sealed static cell results of Fig. 1. This high capacity loss can be mainly attributed to the high rate of air oxidation of the V^{2+} ions in the open reservoir with the large electrolyte surface area to volume ratio used. In practice, this can be minimised by employing an inert gas blanket in the negative electrolyte tank to exclude oxygen and/or by designing the electrolyte reservoirs with a very small surface area to volume ratio to make the air oxidation process diffusion limited. The other side reaction leading to the high loss of capacity is hydrogen evolution during charging. This lowers the conversion of vanadium ions at negative electrode surface particularly at high states-of-charge and with large currents. In practice, action can be taken to prevent evolution of hydrogen by ceasing the charging process at a reasonable state-of-charge limit, although the usable capacity of the VFB would be restricted by such operations.

Unlike the capacity loss caused by the different transfer of vanadium ions across the membrane, the above side reactions cause an electrolyte imbalance that cannot be restored by simple electrolyte remixing but requires either chemical or electrochemical rebalancing to restore capacity loss. An effective control system for cell rebalancing requires a dynamic model that is able to predict the capacity loss due to the above phenomena so that the controller can determine when such rebalancing processes is to be scheduled.

3. Dynamic model development

Mathematical modelling helps with understanding processes and plays an important role in process design, optimization and

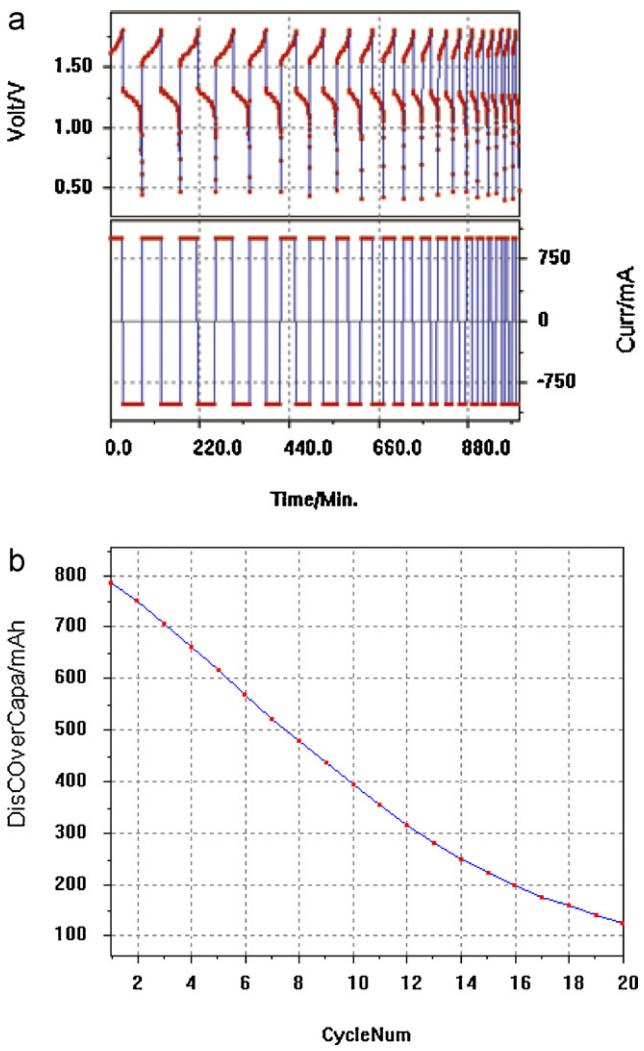

Fig. 2. Performance of a flow cell with perfluorinated cation exchange membrane. (a) Voltage and current curves. (b) Capacity vs. cycle number.

control. Steady-state models represent the static behaviour of the process. In most real situations, however, conditions change with respect to time. Under these circumstances, a dynamic model is required to characterize the transient behaviours of a process over a wide range of conditions. Generally, dynamic modelling can be developed based on the fundamental mechanisms of processes, such as conservations of mass and energy. Meanwhile, assumptions need to be made in order to derive process models with suitable level of details for their purpose by omitting less important phenomena.

As mentioned above, membrane diffusion and side reactions lead to loss of capacity in charge–discharge cycling operation by creating an imbalance in vanadium ions and vanadium ion ratios in the two half-cells. Thus, readjustment of the electrolyte chemistry is required to be implemented periodically so as to recover capacity and achieve desirable performance over many thousands of charge–discharge cycles. A dynamical model is able to help with capacity loss predictions in order to take any necessary electrolyte maintenance. In the development of this dynamic model for the vanadium redox flow battery, the following assumptions were made for the purpose of simplifying the model:

(1) Temperature is assumed constant at room temperature;
(2) Electrolyte flow rate is not taken into account;

(3) Side reactions caused by diffusion of ions across the membrane are instantaneous;
(4) The volumes of both electrolytes remain constant;
(5) The rates of the cell charge–discharge reactions can be described by Faraday's law of electrolysis;
(6) Side reactions (5) and (8) are negligible;
(7) The electrolytes are perfectly mixed;
(8) The proton concentration in each half-cell electrolyte remains constant during charge–discharge cycling.

Based on the above assumptions and molar mass balance, dynamic equations associated with the diffusion terms for all vanadium ions are developed as shown in Eq. (10). Here, diffusion terms for side reactions (5) and (8) are neglected because these two reactions produce V^{3+} and V^{4+} respectively which would further react with V^{5+} and V^{2+} respectively, thus giving the same net reactions as given by reactions (3) and (6). Substituting the resultant concentration terms into the Nernst Equation and adding the cell resistance losses, the cell voltage balance in Eq. (11) can be obtained.

$$\begin{aligned} V_s\frac{dc_2}{dt} &= \pm\frac{iA}{zF} - k_2\frac{c_2}{d}S - 2k_5\frac{c_5}{d}S - k_4\frac{c_4}{d}S \\ V_s\frac{dc_3}{dt} &= \pm\frac{iA}{zF} - k_3\frac{c_3}{d}S + 3k_5\frac{c_5}{d}S + 2k_4\frac{c_4}{d}S \\ V_s\frac{dc_4}{dt} &= \pm\frac{iA}{zF} - k_4\frac{c_4}{d}S + 3k_2\frac{c_2}{d}S + 2k_3\frac{c_3}{d}S \\ V_s\frac{dc_5}{dt} &= \pm\frac{iA}{zF} - k_5\frac{c_5}{d}S - 2k_2\frac{c_2}{d}S - k_3\frac{c_3}{d}S \end{aligned} \tag{10}$$

Nernst Equation:

$$E(t) = E^0 + \frac{RT}{zF}\ln\left[\frac{c_2(t)\times c_5(t)\times c_{H^+}^2(t)}{c_3(t)\times c_4(t)}\right] \tag{11}$$

where

c_2 = concentration of V^{2+} ions, mol L^{-1}
c_3 = concentration of V^{3+} ions, mol L^{-1}
c_4 = concentration of V^{4+} ions, mol L^{-1}
c_5 = concentration of V^{5+} ions, mol L^{-1}
$c_H{}^+$ = concentration of hydrogen ions, mol L^{-1}
k_2 = diffusion coefficient for V^{2+} across the membrane, $dm^2\ s^{-1}$
k_3 = diffusion coefficient for V^{3+} across the membrane, $dm^2\ s^{-1}$
k_4 = diffusion coefficient for V^{4+} across the membrane, $dm^2\ s^{-1}$
k_5 = diffusion coefficient for V^{5+} across the membrane, $dm^2\ s^{-1}$
V_S = volume of half-cell solution, L
i = current density, A cm^{-2}
A = electrode surface area, cm^2
z = number of electrons transferred in reaction (1)
F = Faraday's constant = 96485 C mol^{-1}
d = thickness of membrane, dm
S = membrane area, dm^2
E^0 = standard cell potential, V
T = temperature, K
R = gas constant = 8.314 J mol^{-1} K^{-1}
r = resistance, $\Omega\ cm^2$
'+' and '−' apply to the process of charging and discharging respectively

Due to several ionic equilibria that affect the equilibrium concentrations of all of the ionic species in the in the VFB electrolyte, the concentration of hydrogen ions in the positive half-cell electrolyte is not accurately known. For this reason, the proton concentration is removed from the logarithmic term in the Nernst Equations and combined with the standard potential to produce the formal potential term E^0 that can be determined experimentally. The modified cell voltage balance given by Eq. (12) was therefore used in the development of the dynamic cell voltage model in this study:

$$E(t) = E'_0 + \frac{RT}{zF}\ln\left[\frac{c_2(t)\times c_5(t)}{c_3(t)\times c_4(t)}\right] \tag{12}$$

where E'_0 is the formal cell potential. For 2 M vanadium in 5 M total sulfate electrolyte, the formal potential was measured as 1.4 V at 50% state-of-charge [26].

Table 1
Values of diffusion coefficients for vanadium ions across three different membranes.

Membrane	k_2 ($dm s^{-1}$)	k_3 ($dm s^{-1}$)	k_4 ($dm s^{-1}$)	k_5 ($dm s^{-1}$)
Selemion CMV	3.17×10^{-7}	0.716×10^{-7}	2×10^{-7}	1.25×10^{-7}
Selemion AMV	3.53×10^{-8}	2.18×10^{-8}	0.91×10^{-8}	2.57×10^{-8}
Nafion 115	6.9×10^{-7}	2.54×10^{-7}	5.37×10^{-7}	4.64×10^{-7}

4. Simulation and results

For the simulation carried out in this paper, the following parameters were used in the modelling:

(i) Upper and lower cell voltage limits were set at 1.7 V and 1.1 V for the end of charge and end of discharge cycles respectively.
(ii) Membrane area and electrode surface area were with the same value of 30 dm^2.
(iii) The volume of each half-cell electrolyte solution was 1 L.
(iv) The cell resistance was set at 2 $\Omega\ cm^2$.
(v) Temperature was set to be 298.15 K.
(vi) The total amount of vanadium ions used in the simulation were assumed to be 2 mol L^{-1} in both half-cells, while 0.01 mol L^{-1} of V^{2+} and V^{5+} in conjunction with 1.99 mol L^{-1} of V^{3+} and V^{4+} were set for the initial values of the dynamic model to avoid a zero logarithmic term in the Nernst Equation.

Furthermore, 1.4 V was employed as the formal potential which is the actual open-circuit potential measured at 50% SOC with 2 M vanadium in 5 M total sulfate [26]. The simulations were conducted by switching the charging and discharging processes between the upper and lower cell voltage limits. To investigate different types of membrane with respect to the capacity loss, a current density of 60 mA cm^{-2} was used which is equivalent to 180 A in this case. Three different membranes were employed in the simulation with the diffusion coefficients summarized in Table 1 [5,25]. The values of the Nafion 115 diffusion coefficients reported in [25] were converted from units of $cm^2\ min^{-1}$ to $dm s^{-1}$ by multiplying for the membrane's thickness, 127 microns and by the corresponding conversion factor to obtain units of $dm s^{-1}$ as summarised in Table 1.

4.1. Case 1: Vanadium ion diffusion with no side reactions

4.1.1. Selemion CMV membrane

The vanadium ion diffusion coefficients for Selemion CMV cation-exchange membrane were firstly employed in the simulation. In Fig. 3 it shows the capacity change for the VFB as a function of cycle number for 200 charge–discharge cycles. As seen, the capacity drops 15% after 200 cycles. The corresponding discharging time variation can be observed in Fig. 4 in which the initial charge–discharge curves are compared with those for cycles 97–100 and 197–200. This gradual decrease in discharge time with continued cycling is due to the differential transfer of vanadium ions across the membrane that produces an imbalance in the vanadium ion concentration in the two half-cells. This can be seen in Fig. 5 where a build-up in total vanadium concentration in the positive half-cell electrolyte along with the corresponding loss in the negative electrolyte is shown.

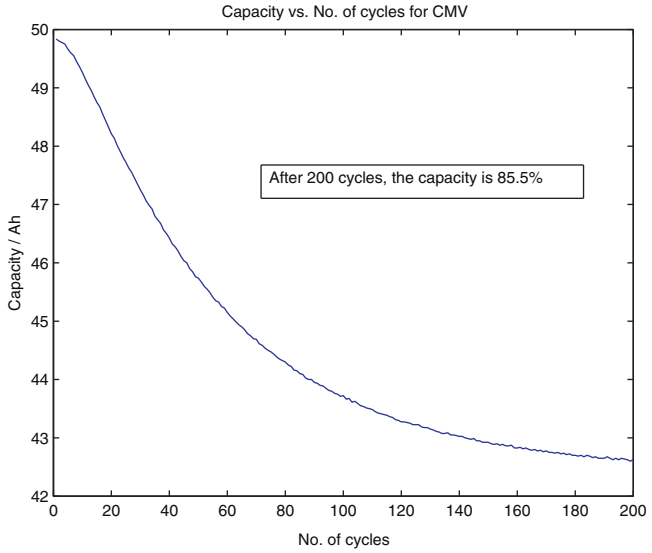

Fig. 3. Capacity vs. No. of cycles for 200 cycles for CMV membrane.

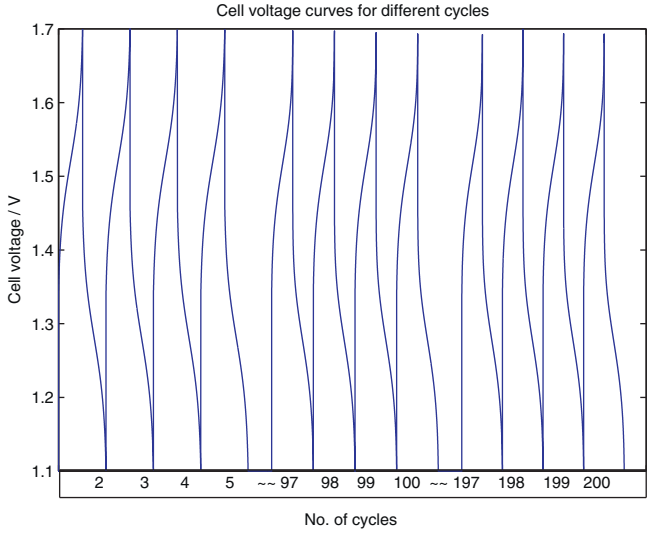

Fig. 4. Comparison of cell voltage curves for different cycles for CMV membrane.

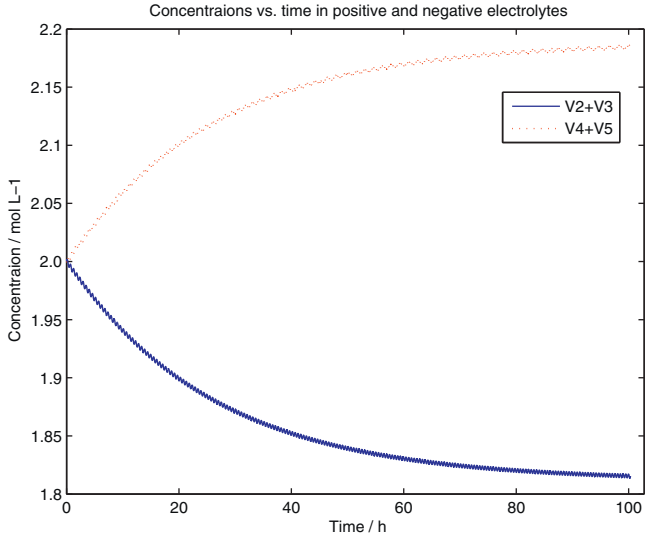

Fig. 5. Concentrations of positive and negative electrolytes vs. time for 200 cycles for CMV membrane.

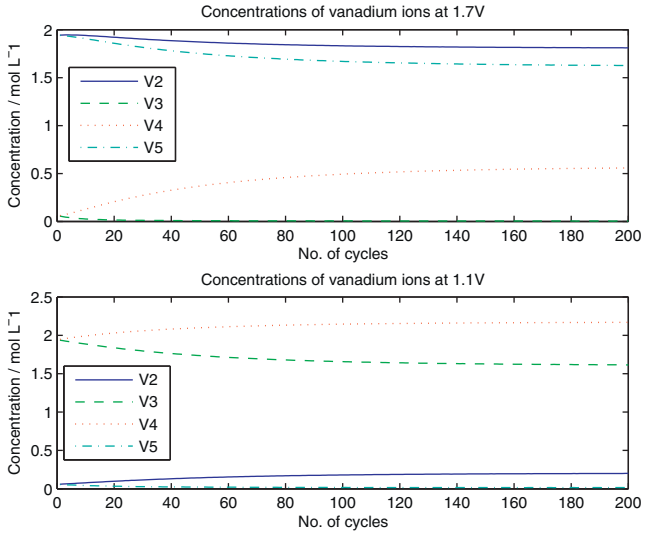

Fig. 6. Vanadium ion concentrations vs. cycle number at 1.7 V and 1.1 V for CMV membrane.

Further concentration profiles as a function of cycle number at the upper and lower voltage limits (corresponding to top of charge and end of discharge respectively) can be observed in Fig. 6. This shows that the concentration of V^{4+} increases while the other three vanadium ions experience a slight decrease over time. This can be attributed to the order of diffusion coefficient values which is $V^{2+} > V^{4+} > V^{5+} > V^{3+}$ such that given a certain amount of V^{2+} going through the membrane, more V^{5+} would be consumed according to the reaction shown in Eq. (3), producing even more V^{4+} in the positive electrolyte. Similarly, as V^{5+} diffuses across the membrane, it reacts with V^{2+} ions, producing V^{3+} according to the self-discharge reaction given in Eq. (6). In addition, it is seen from these equations that no V^{2+} and V^{5+} can be produced by the self-discharge side reactions. Thus, the concentrations of V^{2+} and V^{5+} show a decrease with the number of cycles at the upper limit of voltage in Fig. 6. Finally, a decreasing trend in concentration change with respect to V^{2+} is observed by comparing the two plots in Fig. 6, which is in accordance with the capacity loss shown in Fig. 3. It is interesting to note that a rapid decrease in both the ion concentrations and cell capacity occurs in the first 100 cycles, but these changes slow down and approach steady state at around 200 cycles.

4.1.2. Selemion AMV membrane

The anion exchange membrane Selemion AMV was also used in the simulation for comparison. Compared with the cation exchange membrane Selemion CMV, the diffusion coefficients for all except the V^{3+} ions are around an order of magnitude smaller, while the order of the diffusion rates is $V^{2+} > V^{5+} > V^{3+} > V^{4+}$. This difference in the diffusion rates compared with CMV can be explained in terms of the fact that vanadium cations are repelled by the anion exchange membrane, giving rise to much smaller diffusion coefficients.

Fig. 7 shows that the capacity drops about 19% after 200 cycles resulting in a decrease trend of charge–discharge cycling time observed in the cell voltage versus time curve. This is also due to the diffusion effect within the cells that affects the long term cycling performance. Interestingly, the capacity with this membrane has dropped more than that of CMV shown above after 200 charge–discharge cycles in spite of the smaller diffusion rates for AMV. Comparing Fig. 7 with Fig. 3, it is seen that the initial rate of cell capacity decline is much smaller in the case of the AMV membrane, consistent with the lower diffusion coefficients compared with CMV. On the other hand, comparing Fig. 8 with Fig. 6 it is seen that despite the relatively high initial rate of capacity loss

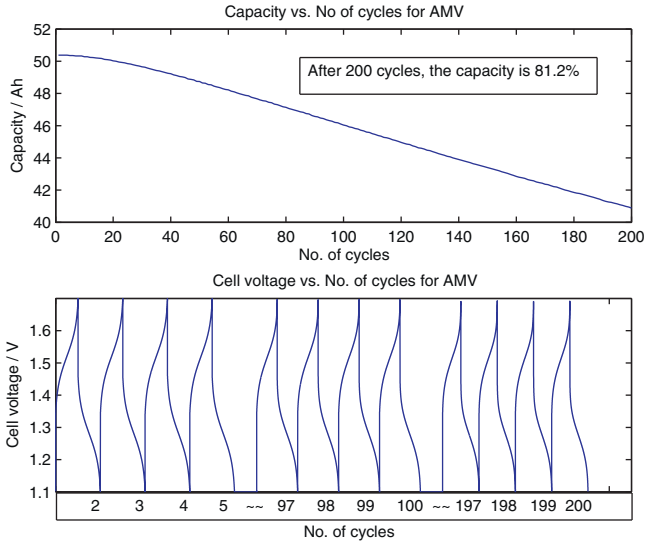

Fig. 7. Capacity and cell voltage vs. No. of cycles for 200 cycles for AMV membrane.

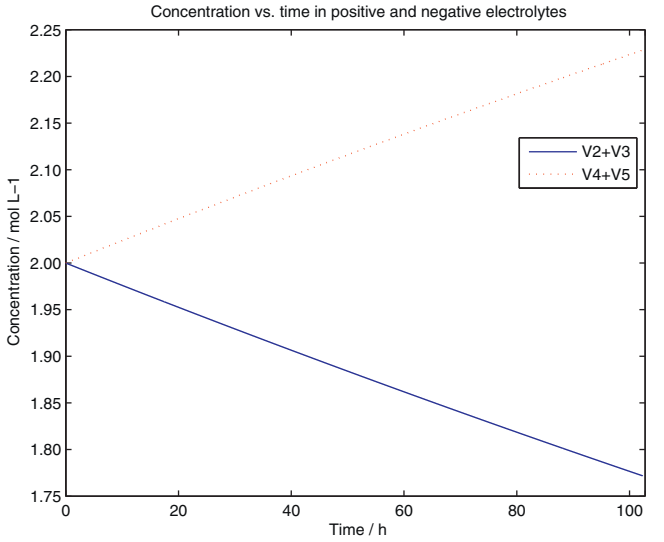

Fig. 9. Concentration of positive and negative electrolytes vs. time for 200 cycles for AMV membrane.

with the CMV membrane, steady state is achieved after within 200 cycles, resulting in a relatively small capacity loss compared with AMV where the concentrations of the vanadium ions continue to change without reaching steady state. Therefore, the differential transfer of vanadium ions across the AMV membrane continues to produce an imbalance in the total vanadium ion concentrations in the cell as shown in Fig. 9, leading to a continuing decline in the cell capacity. As a matter of fact, in the absence of other factors such as side reactions, the vanadium ion concentrations along with the capacity should reach a steady state after a certain number of charge–discharge cycles, although this is not observed within the 200 cycles simulated here. An important observation from these simulations, however, has been that not only are the absolute values of the different diffusion coefficients important in determining the rate of capacity decline, but in the absence of other factors, the relative values for the four different vanadium ions will also play an important role in the attainment of steady state in cell capacity. It is also interesting to note that as in the case of the CMV cation exchange membrane, with the values of the four vanadium ion diffusion rates used here, a steady build-up of total vanadium concentration is observed in the positive half-cell with a corresponding dilution in the negative half of the vanadium redox flow cell employing the AMV anion exchange membrane.

4.1.3. Nafion 115 membrane

The diffusion coefficients of vanadium ions across Nafion 115 membrane have been measured and reported in [25] with a decreasing order of $V^{2+} > V^{4+} > V^{5+} > V^{3+}$. As shown in Fig. 10 the capacity is 89.4% after 200 charge–discharge cycles. It is worth noting that the main capacity loss has occurred in the first 100 charge–discharge cycles. This is due to the larger diffusion coefficients of Nafion 115 membrane that contribute to a faster convergence of vanadium ion concentrations at upper and lower voltage limits as observed in Fig. 11. Additionally, it is also worth noting from Fig. 11 that the concentration of V^{2+} is less than that of V^{5+} at upper limit of 1.7 V while V^{4+} is less than V^{3+} at lower limit of 1.1 V which differs from the trend observed for CMV membrane although the order of diffusion rates are same. Therefore, it is reasonably concluded that different relative values of diffusion coefficients will result in different half-cell vanadium

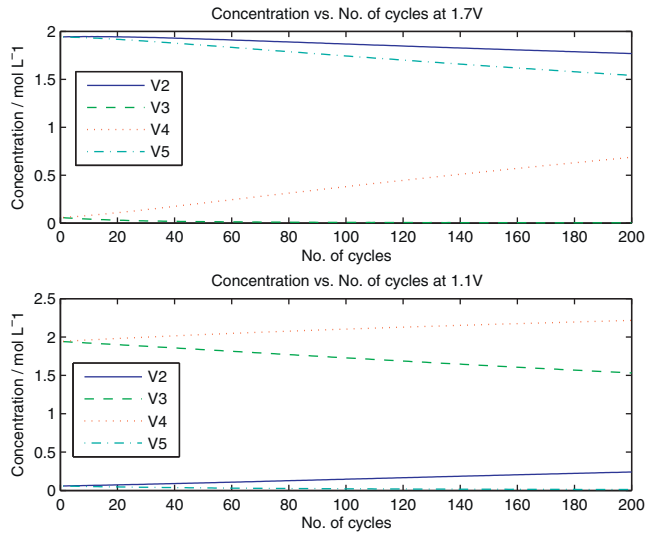

Fig. 8. Vanadium ion concentrations vs. No. of cycles at 1.7 V and 1.1 V for 200 cycles for AMV membrane.

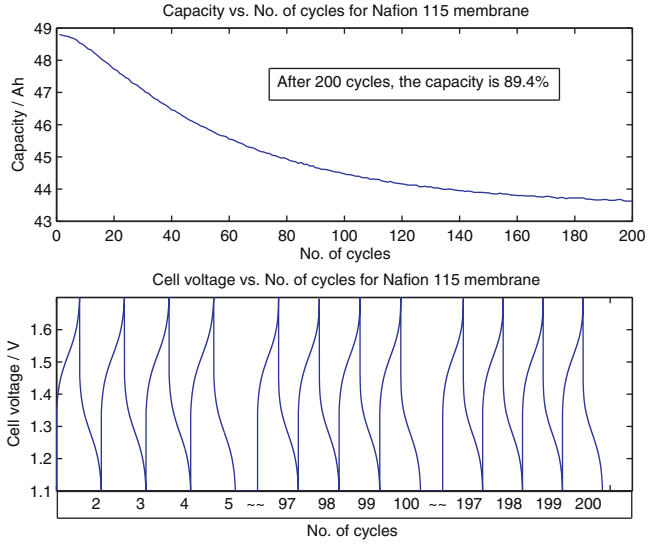

Fig. 10. Capacity and cell voltage vs. No. of cycles for 200 cycles for Nafion 115 membrane.

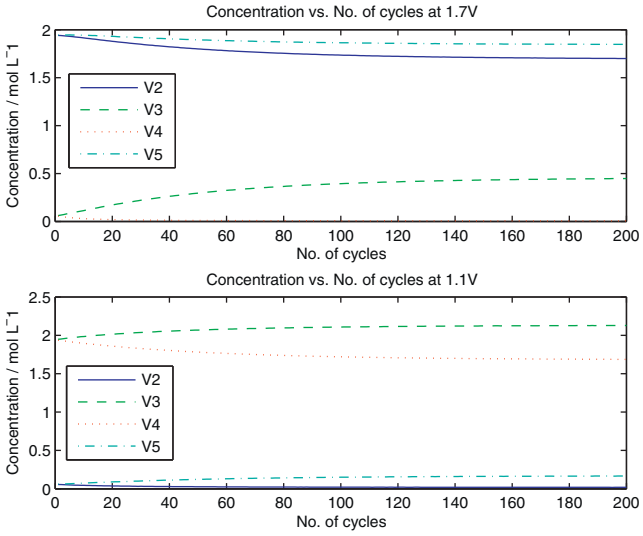

Fig. 11. Vanadium ion concentrations vs. No. of cycles at 1.7 V and 1.1 V for 200 cycles for Nafion 115 membrane.

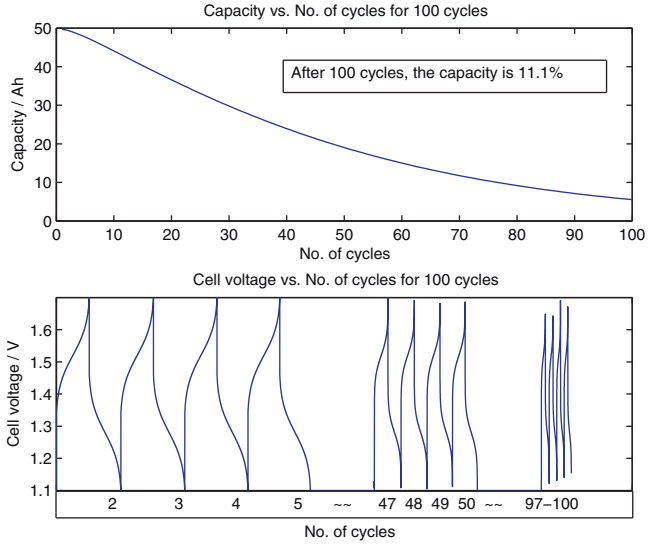

Fig. 13. Capacity and cell voltage vs. cycle number for CMV membrane with 0.98 current efficiency factor for V^{2+} charging reaction.

accumulations in the simulation despite the same order in relative diffusion rates. Finally, referring to Figs. 5 and 12, there is an accumulation of vanadium in the negative half-cell for the Nafion 115 membrane, opposite to the observed trend for CMV. In the case of Nafion, the total vanadium concentration in the negative half-cell solution shows an increase of approximately 7% after 200 charge–discharge cycles and the concentrations of each ion in the two electrolytes tend to reach steady-state within this time-frame. Once again, it is apparent that not only are the magnitudes and order of the four diffusion coefficients important in determining the rate of capacity loss and attainment of steady state, but in the absence of other factors, the relative values will also determine the direction of vanadium accumulation in the cell.

4.2. Case 2: effect of side reactions on capacity loss

Side reactions inevitably occur in all electrochemical energy storage systems, especially during the process of charging, thereby leading to further capacity loss during operation of the VFB. The effect of air oxidation of V^{2+} and hydrogen evolution on cell capacity was simulated here by inserting a current efficiency factor into the charging current for the V^{2+} and V^{3+} mass balance equations in the dynamic model. The Selemion CMV and Nafion 115 membranes were employed in the simulation to investigate the effects on performance.

4.2.1. Selemion CMV membrane

Initially, a factor of 0.98 was used to simulate the side reaction effect on capacity for the CMV membrane. Fig. 13 shows the capacity has dropped to 11% of the original capacity after only 100 charge–discharge cycles because of the side reactions in the negative half-cell. This is further highlighted by the corresponding variation in the charge–discharge voltage curves that also reflect the dramatic capacity loss during the first 100 cycles. Correspondingly, a continued decrease in V^{2+} concentration during cycling can be observed in Fig. 14, showing that a 2% current efficiency loss caused by side reaction will lead to a capacity loss of approximately 89% after 100 cycles. For comparison, a current efficiency factor of 0.9 was also employed in the simulation. As shown in Fig. 15, the

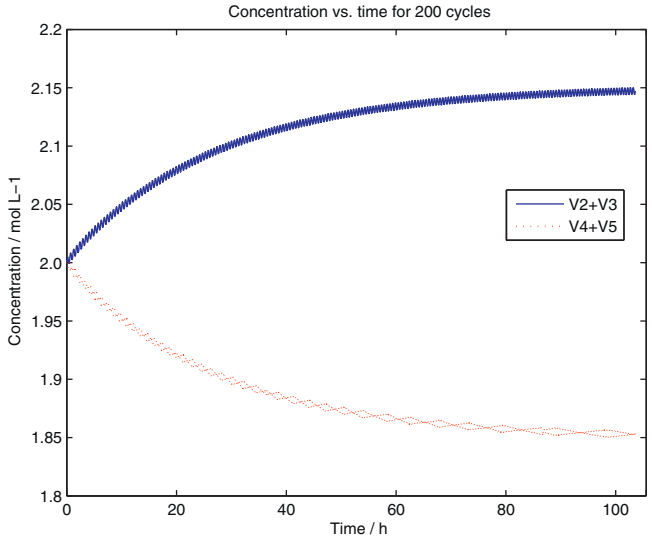

Fig. 12. Concentrations of positive and negative electrolytes vs. time for 200 cycles for Nafion 115 membrane.

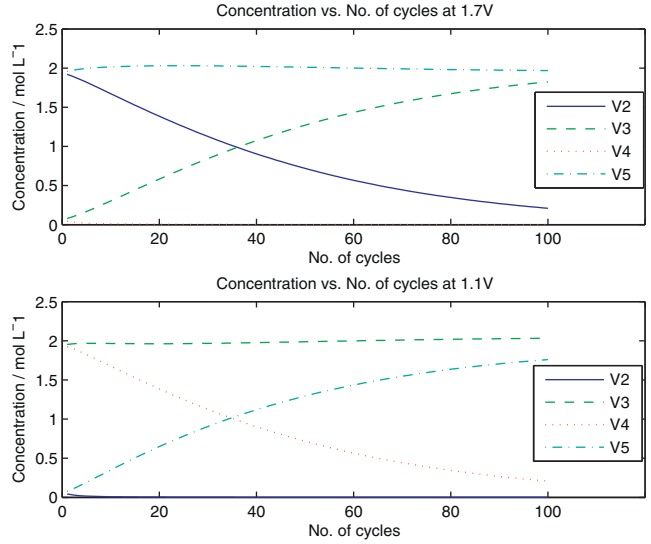

Fig. 14. Vanadium ion concentrations vs. cycle number at 1.7 V and 1.1 V for CMV membrane with 0.98 current efficiency factor for V^{2+} charging reaction.

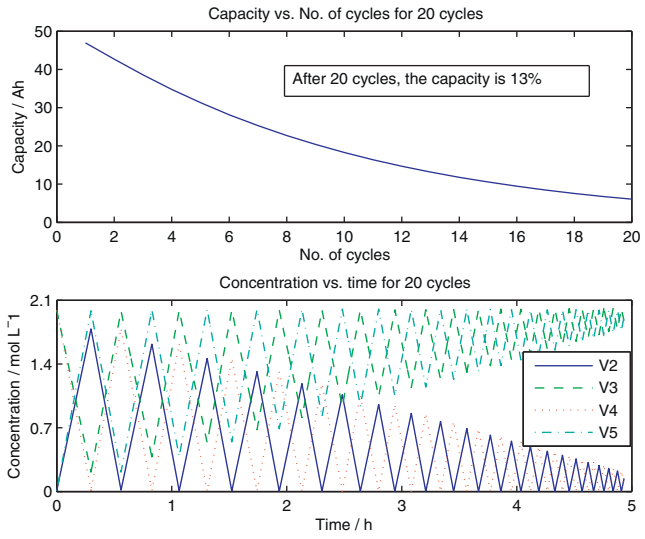

Fig. 15. Capacity and concentration curves for 20 cycles for CMV membrane with 0.9 current efficiency factor for V^{2+} charging reaction.

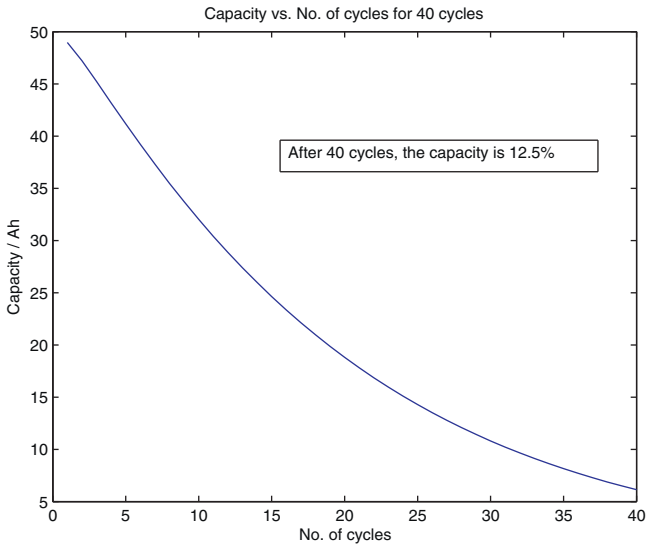

Fig. 17. Capacity vs. cycle number for 40 cycles for CMV membrane with 0.95 current efficiency factor for V^{2+} charging reaction.

capacity loss is approximately 87% after only 20 charge–discharge cycles. Fig. 16 further shows the variations of voltage and current curves for 20 cycles which has a trend similar to the experimental results shown in Fig. 2a. Fig. 2b shows a capacity loss of approximately 86% after 20 cycles for the small laboratory flow cell. As both experiment and simulation employed cation exchange membrane and results were extremely similar, it is reasonable to conclude that side reactions caused by the open electrolyte reservoirs and large current density led to 10% loss of current efficiency in the negative half-cell for the laboratory flow cell. It is also seen in Fig. 15 that the concentration of V^{2+} at the end of 20 cycles is five times smaller than that observed in Fig. 14 at the 20th cycle. Therefore, it is reasonable to predict that 40 charge–discharge cycles might be required for the same amount of capacity loss with a current efficiency factor of 0.95. This is in agreement with the simulation result given by Fig. 17.

4.2.2. Nafion 115 membrane

To start with, a charging current efficiency of 98% for the negative electrode reaction was used in effort to simulate the effect of gas side reaction in Nafion 115 membrane. Fig. 18 shows that the capacity has dropped dramatically for 40 charging–discharging cycles which can be observed from the decreasing charging–discharging time in Fig. 19 as well. Furthermore, referring to Fig. 20 V^{2+} has experienced a continuous decrease as a function of cycle number at the upper voltage limit due to the loss of current efficiency caused by the gas side reaction that would lower the conversion of V^{2+} during charging. Correspondingly, V^{5+} will increase as a function of cycle number in discharging process which can be observed at the lower voltage limit in Fig. 20. Finally it is seen from Fig. 21 that rather than reaching a relative steady state as shown with 100% current efficiency in the previous case study, the vanadium ions have kept accumulating in the negative half-cell electrolyte while decreasing in the positive electrolyte accordingly as a consequence of the gas side reactions. It is worth noting that this predicted trend does not match the results from a recent experimental study of a kilo-watt scale VFB system with Nafion 115 membrane in which the accumulation of vanadium ions was seen to occur in the positive half-cell electrolyte [25]. It should be noted, however, that a low SOC range was employed

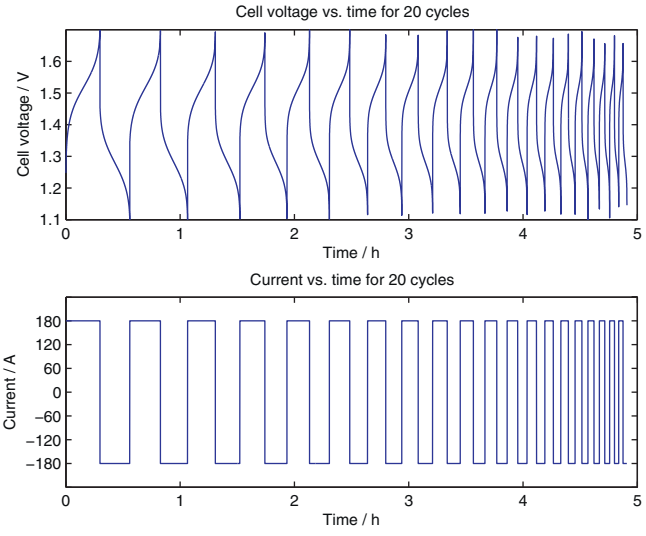

Fig. 16. Cell voltage and current vs. time for 20 cycles for CMV membrane with 0.9 current efficiency factor for V^{2+} charging reaction.

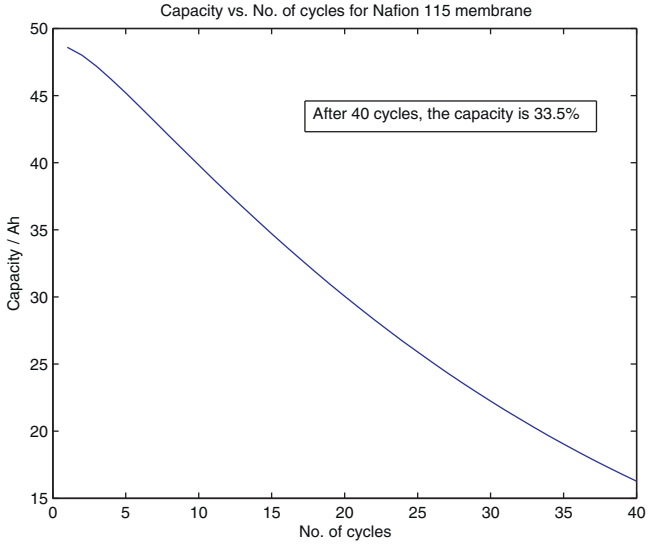

Fig. 18. Capacity vs. cycle number for 40 cycles for Nafion 115 membrane with 0.98 current efficiency factor for V^{2+} charging reaction.

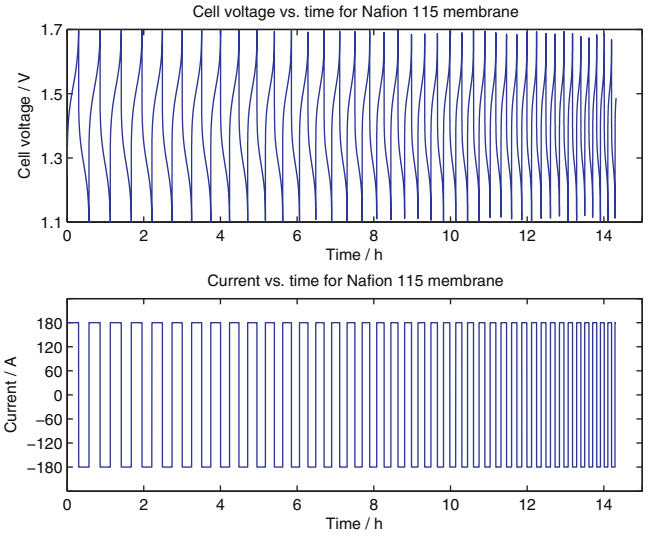

Fig. 19. Cell voltage and current vs. time for 40 cycles for Nafion 115 membrane with 0.98 current efficiency factor for V^{2+} charging reaction.

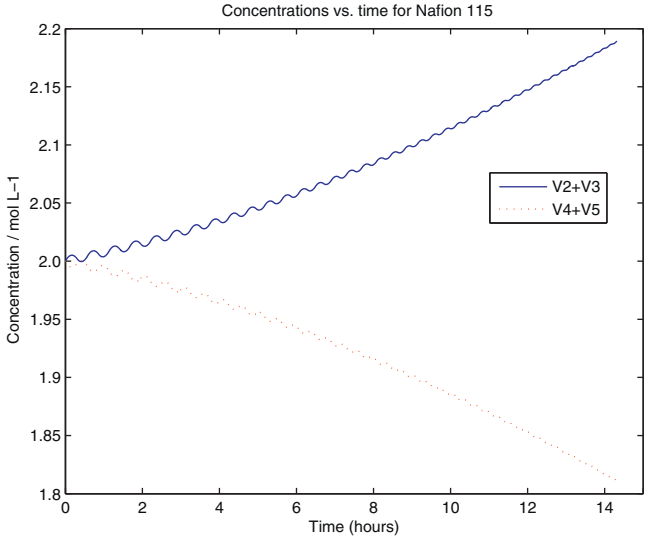

Fig. 21. Concentrations of positive and negative electrolytes vs. time for 40 cycles for Nafion 115 membrane with 0.98 current efficiency factor for V^{2+} charging reaction.

in [25] such that side reactions would be minimised during charging, while considerable volumetric transfer was also observed from the negative into the positive half-cell electrolyte reservoirs. This bulk electrolyte transfer has been attributed to water transfer associated with osmotic pressure effects across the membrane that also drag bulk electrolyte from the negative to the positive half-cell [13,14,25]. Furthermore, the difference in conditions between the present simulation results and the experimental study in [25] makes direct comparison difficult. What is clear, however, is that volumetric transfer is very significant in the VFB and this phenomenon will greatly affect the net accumulation of vanadium ions in the VFB system. A more accurate dynamic model should therefore include the effect of variable electrolyte volume during charge–discharge cycling of the VFB. The dynamic model which accounts the volumetric transfer is currently under investigation.

5. Discussion

Despite the ability to use the dynamic model for prediction of loss of capacity under specified operating conditions in the VFB, it is still worth to investigate the potential factors that restrict the accuracy of the model and further improve performance prediction.

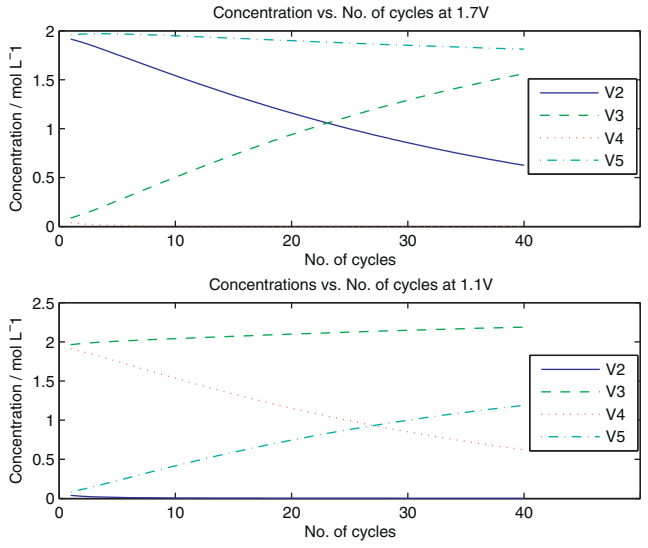

Fig. 20. Vanadium ion concentrations vs. cycle number at 1.7 V and 1.1 V for Nafion 115 membrane with 0.98 current efficiency factor for V^{2+} charging reaction.

5.1. The effect of diffusion coefficients

First of all, considerable errors can arise from the experimental procedures used by different groups to measure diffusion coefficients of the different vanadium ions, and these will have a considerable influence on the accuracy of any prediction. In particular, V^{2+} ions are always difficult to study because of their extreme sensitivity to air which converts V^{2+} to V^{3+} making accurate measurements very difficult. In reality, membrane aging will also change membrane properties, leading to higher or lower permeability of the vanadium ions depending on degree of swelling or fouling during operation. As a result, the initial diffusion rate measurements from static diffusion tests will not accurately describe the real ion diffusion effects on self-discharge and ion accumulation during long-term cycling and operation. In addition, the diffusion rates also vary with temperature. As the cells are being cycled, the temperature of the electrolytes will increase as a result of the reactions and ohmic losses in the cells. This will gives rise to the swelling for membrane and further increase the diffusion rate of all the vanadium ions or even change the order of diffusion rates recorded in the experiment. As a matter of fact, extra simulations have shown that incorporating different relative values of diffusion coefficients into the simulation could possibly result in different trends even when the same order of the diffusion rates is maintained. Thus, a dynamic diffusion rate based on battery cycling experiments would be required in order to simulate a more realistic situation in terms of the ion diffusion within the cells. Furthermore, additional factors such as electric field and co-existence of different ions during charge–discharge cycling also affect the accuracy of the measured diffusion coefficients and highlight the need for further experimental measurement under conditions that simulate real cell operation.

5.2. The effect of flow rate and volumetric transfer

Flow rate plays an important role in real-life systems since insufficient flow rate will limit the reactions within the half-cells and reduce the cycling time, thereby leading to loss of capacity that is not predicted by the present model. Differential flow rates or a high different pressure drop across the membrane could also cause significant bulk electrolyte transfer from one half-cell to the other

that swamps the effects of ion transfer, leading to further inconsistencies between experimental and simulated trends. Moreover, the water carried by the vanadium ions and dragged by the proton across the membrane can also have a slight impact on the imbalance of the two half-cell electrolytes and this has been neglected in the present model. Last but not least, water is also associated with the charge–discharge reactions in the positive half-cell electrolyte where water is consumed and generated during the charging and discharging processes as shown in Eq. (1). In real-life VFB systems therefore, the volumes of the two half-cell electrolytes keep changing during charge–discharge cycling, but laboratory observations show that a stead state is reached after a certain number of cycles depending on the type of membrane and cycling conditions used. Nevertheless, the exact volumes of the electrolytes in both half-cells as a function of time are difficult and even impossible to determine mathematically due to the complicated equilibria in the electrolytes that make it difficult to accurately calculate the total ionic strength of the solutions during cycling and the resultant changes in osmotic pressure. In the present case, the accuracy of the model will be affected by the assumption of constant electrolyte volume. But given the complexity of the solution chemistry, theoretical predictions would be very inaccurate [27]. Further studies on the effect of volumetric transfer on the model should therefore incorporate experimental measurements of electrolyte volume changes during charge–discharge cycling of a VRB battery system in order to improve the accuracy of prediction. Unfortunately very little data on dynamic volume changes is available in the literature, so for the purpose of the present simulation, this effect has been neglected.

5.3. The effect of concentration of hydrogen ions

The concentration of hydrogen ions in the positive half-cell electrolyte varies during charge–discharge cycling due to the transfer of hydrogen ions across the membrane for charge balance as well as changes associated with the redox reaction at the positive electrode. As discussed above, the chemistry of the vanadium electrolytes is very complex with several ionic equilibria interacting to change the equilibrium concentration of hydrogen ions in the positive electrolyte during cycling [27]. Given that equilibrium constants for many of these reactions are not accurately known, accurate calculation of equilibrium proton concentrations during cycling is very difficult. Changes in the hydrogen ion concentration during change-discharge cycling are expected to affect the Nernst potential for the positive half-cell reaction and therefore the shape of the dynamic voltage curve produced by the simulation. In order to understand the magnitude of this effect, the cell voltage curve was modelled for both situations of constant and varying proton concentration. Assuming that the electrolyte contains 2 M vanadium in 2.5 M total sulfate, for instance, the following proton mass balance for the positive half-cell electrolyte is incorporated into the Nernst Equation in order to calculate the effect of varying hydrogen ion concentration on the theoretical cell voltage curve:

$$[H^+] = [H^+]_0 + 2 \times SOC \quad (13)$$

In Eq. (13), it is assumed that during charging, one mole proton transfers across the membrane from the positive half-cell to the negative half-cell for every mole of vanadium ions reacting, while 2 moles of protons are also produced by reaction (1). Assuming that the hydrogen ions are not affected by other ionic equilibria in the solutions, Eq. (13) can be incorporated into the Nernst Equation to estimate the effect of varying hydrogen concentration in the positive half-cell electrolyte on the dynamic cell voltage. As seen in Fig. 22, the voltage difference between the variable and constant proton concentration cases varies from zero to 30 mV as a function of state of charge. Importantly however, while affecting the shape of the dynamic cell voltage curve, the variation in hydrogen ion concentration during charge–discharge cycling has no effect on cell capacity that is the main purpose of the present dynamic model.

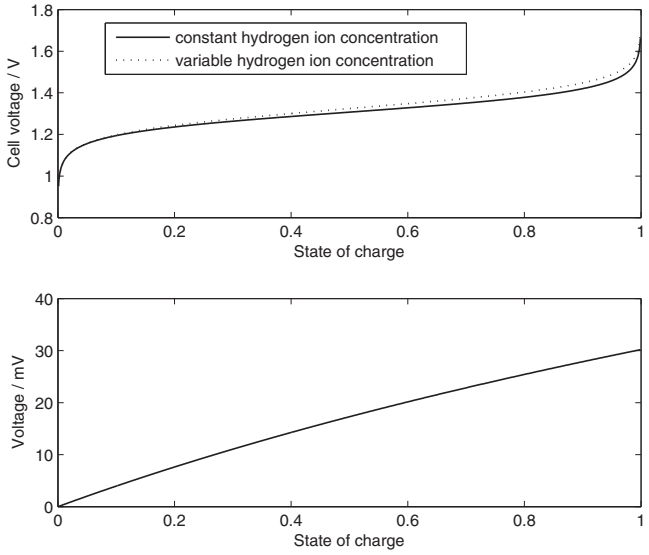

Fig. 22. Comparison of theoretical cell voltages calculated by assuming constant and variable hydrogen ion concentration in the Nernst equation.

5.4. Other effects and preventive actions

Apart from the factors mentioned above, other factors such as charge–discharge current magnitude and the effect of shunt currents in a bipolar stack will also have a considerable influence on cell capacity and further add to discrepancies between experimental and simulated trends. Hence, such additional factors need to be included in the further development of the model so as to not only perform a more reasonable capacity prediction, but provide deeper insight into the real-life system operation as well. From the above case studies, in the meanwhile, it is seen that side reactions in negative electrolyte during charging could have a significant impact on capacity loss if appropriate operational limits and battery design considerations are not implemented. In practical VFB systems, however, many actions can be taken to eliminate the effect of side reactions on capacity loss. Examples include the employment of an inert gas or other type of air blanket within the negative electrolyte reservoir to minimise air oxidation of V^{2+}, avoiding overcharging and elimination of electrolyte impurities that will catalyse hydrogen evolution. None of them can, however, completely eliminate the influence of side reactions over many thousands of cycles. As such, the prediction of capacity loss will help with automated electrolyte management decisions for periodic electrolyte rebalancing to maintain and restore capacity.

6. Conclusions

A dynamic model based on molar mass balance equations for the four vanadium species in the all-vanadium redox battery has been developed and presented in this paper. Using the Nernst Equation, a dynamic model for cell potential has been developed and used to simulate and predict the capacity loss caused by diffusion of vanadium ions across the membrane as well as side reactions in the negative half-cell over long term charge–discharge cycling and operation of the VFB. Three membranes with different sets of reported diffusion coefficients have been employed in the simulation. The results have shown that the rate of capacity loss versus cycle number under preset limits of cell voltage is influenced by

both the absolute and relative magnitudes of the different vanadium ion diffusion coefficients. In the absence of side reactions, larger diffusion rates tend to level off faster and attain a steady-state capacity over a smaller number of charge–discharge cycles. Additionally, the concentration variation of vanadium ions and the direction of net vanadium accumulation are associated with the relative values of the diffusion coefficients of the four different vanadium ions in the VFB. With respect to side reactions, air oxidation of V^{2+} and evolution of hydrogen during charging will result in significant capacity loss during ongoing cycling. Even a small loss of current efficiency for the negative half-cell reactions will produce a dramatic drop in capacity, highlighting the importance of good voltage control to reduce gassing side reactions and negative electrolyte blanketing to prevent air oxidation of V^{2+}.

The dynamic model will play an essential role in predicting the scheduling of periodic electrolyte rebalancing in the VFB so as to restore the capacity loss caused by ion diffusion and side reaction effects, thereby enabling long term charge–discharge cycling to be carried out without a large loss of capacity. Besides, this study highlights the importance of rebalance cell technology as well as advanced battery control systems that can monitor electrolyte imbalance and maintain electrolyte chemistry in order to manage the long-term operation and performance of the VFB. Laboratory observations have, however, shown that other factors such as volumetric transfer of solutions from one half-cell to the other can also be caused by differential pumping pressure across the membrane and this will also give rise to an additional impact on capacity and performance of the VFB. These issues will be taken into account in the further development of the VFB dynamic modelling that continues to be evolved. Furthermore, the effect of electrolyte flow rate on vanadium ion concentrations in the cells, which in turn influences the charge–discharge cycling time and capacity has also been ignored in this paper, but will be incorporated into the refined model to better simulate the capacity and performance of real VFB systems. Further investigation with respect to all the above issues is in progress and results will be presented in a future publication.

References

[1] M. Skyllas-Kazacos, G. Kazacos, G. Poon, H. Verseema, Int. J. Energy. Res. 34 (2010) 182–189.
[2] M. Skyllas-Kazacos, Encyclopedia of Electrochemical Power Sources, Elsevier, Amsterdam, 2009, pp. 444–453.
[3] M. Skyllas-kazacos, M. Rychick, R. Robins, All-vanadium redox battery, United States Patent, No. 4,786,567 (1988).
[4] M. Skyllas-Kazacos, D. Kasherman, D.R. Hong, M. Kazacos, J. Power Sources 35 (1991) 399–404.
[5] F. Grossmith, P. Llewellyn, A. Fane, M. Skyllas-Kazacos, Proceedings of Symposium on Energy Storage: Load Levelling and Remote Applications, The Electrochemical Society, 1988, p. 11.
[6] S.C. Chieng, M. Kazacos, M. Skyllas-Kazacos, J. Power Sources 39 (1992) 11–19.
[7] S.C. Chieng, M. Kazacos, M. Skyllas-Kazacos, J. Membr. Sci. 75 (1992) 81–91.
[8] T. Mohammadi, M. Skyllas-Kazacos, J. Membr. Sci. 98 (1995) 77–87.
[9] T. Mohammadi, M. Skyllas-Kazacos, J. Power Sources 56 (1995) 91–96.
[10] T. Mohammadi, M. Skyllas-Kazacos, J. Membr. Sci. 107 (1995) 35–45.
[11] T. Mohammadi, M.S. Kazacos, J. Appl. Electrochem. 27 (1997) 153–160.
[12] T. Mohammadi, M.S. Kazacos, J. Power Sources 63 (1996) 179–186.
[13] T. Sukkar, M. Skyllas-Kazacos, J. Membr. Sci. 222 (2003) 235–247.
[14] T. Sukkar, M. Skyllas-Kazacos, J. Membr. Sci. 222 (2003) 249–264.
[15] T. Sukkar, M. Skyllas-Kazacos, J. Appl. Electrochem. 34 (2004) 137–145.
[16] J. Xi, Z. Wu, X. Qiu, L. Chen, J. Power Sources 166 (2007) 531–536.
[17] Q. Luo, H. Zhang, J. Chen, P. Qian, Y. Zhai, J. Membr. Sci. 311 (2008) 98–103.
[18] C. Jia, J. Liu, C. Yan, J. Power Sources 195 (2010) 4380–4383.
[19] A.A. Shah, M.J. Watt-Smith, F.C. Walsh, Electrochim. Acta 53 (2008) 8087–8100.
[20] H. Al-Fetlawi, A.A. Shah, F.C. Walsh, Electrochim. Acta 55 (2009) 78–89.
[21] H. Al-Fetlawi, A.A. Shah, F.C. Walsh, Electrochim. Acta 55 (2010) 3192–3205.
[22] A.A. Shah, H. Al-Fetlawi, F.C. Walsh, Electrochim. Acta 55 (2010) 1125–1139.
[23] M. Li, T. Hikihara, IEICE Trans. Fund. Electron. Commun. Comput. Sci. E91-A (2008) 1741–1747.
[24] D. You, H. Zhang, J. Chen, Electrochim. Acta 54 (2009) 6827–6836.
[25] C. Sun, J. Chen, H. Zhang, X. Han, Q. Luo, J. Power Sources 195 (2010) 890–897.
[26] M. Skylas-Kazacos, M. Kazacos, R. Wegner, R. Burford, G. Lin, Final Report NSW, Dept. of Minerals & Energy, 1991, pp. 200.
[27] C. Blanc, Modelling of a vanadium redox flow battery electricity storage system, Ph.D. Thesis, EPFL, Switzerland, 2009.